ENVIRONMENTAL RESEARCH
LETTERS

LETTER • OPEN ACCESS

Responses of compound daytime and nighttime warm-dry and warm-humid events to individual anthropogenic forcings

ENVIRONMENTAL RESEARCH
LETTERS

OPEN ACCESS

RECEIVED
24 January 2022

REVISED
3 June 2022

ACCEPTED FOR PUBLICATION
13 July 2022

PUBLISHED
22 July 2022

LETTER

Responses of compound daytime and nighttime warm-dry and warm-humid events to individual anthropogenic forcings

Felicia Chiang[1,*], **Benjamin I Cook**[1,2], **Sonali McDermid**[1,3], **Kate Marvel**[1,4], **Gavin A Schmidt**[1], **Larissa S Nazarenko**[1,4] **and Maxwell Kelley**[1,5]

[1] NASA Goddard Institute for Space Studies, New York, NY, United States of America
[2] Lamont-Doherty Earth Observatory, Columbia University, Palisades, NY, United States of America
[3] Department of Environmental Studies, New York University, New York, NY, United States of America
[4] Center for Climate Systems Research, Columbia University, New York, NY, United States of America
[5] SciSpace LLC, New York, NY, United States of America
[*] Author to whom any correspondence should be addressed.

E-mail: felicia.chiang@nasa.gov

Keywords: anthropogenic forcings, compound events, climate extremes

Supplementary material for this article is available online

Abstract

Daytime heat is often associated with reduced soil moisture and cloud cover, while nighttime heat is connected to high humidity and increased cloud cover. Due to these differing mechanisms, compound daytime and nighttime heat events may respond differently to major anthropogenic forcings (greenhouse gases, anthropogenic aerosols, land-use and land-cover change). Here, we use GISS ModelE2.1-G historical single-forcing runs from 1955 to 2014 to examine how individual anthropogenic forcings affect compound heat events—specifically warm daytime and nighttime temperatures compounded with dry precipitation or high humidity conditions. We show that greenhouse gases alone amplify the natural frequency of warm-dry events by 1.5–5 times and warm-humid events by 2–9 times in tropical and extratropical latitudes. Conversely, aerosols and land-use/land-cover change reduce the frequency of these events, resulting in more modest increases and in some regions, declines, in the historical 'all-forcings' scenario. Individually, aerosol effects are stronger and more widespread compared to land-use, oftentimes reducing the natural frequency of these events by 60%–100%. The responses of these compound events are primarily driven by changes in daytime and nighttime temperatures through large-scale warming via greenhouse gases and cooling from aerosols and land-use/land-cover change. However, changes in warm-dry events are amplified in regions with concurrent precipitation declines (e.g. Central America, Mediterranean regions) and warm-humid events are amplified by global concurrent humidity increases. Additionally, we find differences between daytime and nighttime compound responses in the historical experiment that can be traced back to the individual forcings. In particular, aerosols produce a greater cooling effect on daytime relative to nighttime temperatures, which notably results in a historical reduction of Northern Hemisphere daytime warm-dry events relative to natural conditions. Our analysis provides a more comprehensive understanding of the significant impacts of different anthropogenic climate forcings on daytime and nighttime warm-dry and warm-humid events, informing future risk and impact assessments.

1. Introduction

Human activities have caused regional and large-scale changes in the Earth's climate through several anthropogenic forcings (IPCC 2021). Rising greenhouse gas concentrations have driven significant global temperature increases, changes in precipitation patterns, and the increasing frequency and intensity of extreme events, including heatwaves, extreme rainfall, and droughts (Hegerl *et al* 1997, Christidis *et al* 2005, Seneviratne *et al* 2012, Easterling *et al* 2016, Marvel *et al* 2019). Anthropogenic aerosols have cooled temperatures by increasing regional albedo levels (Charlson *et al* 1992). Aerosols have also

been hypothesized to influence large-scale circulation changes through asymmetrical surface temperature changes, resulting in late 20th century drying in Northern Hemisphere monsoonal regions (Bollasina *et al* 2011, Polson *et al* 2014). Moreover, land cover and land management practices have driven changes in regional climate conditions. Irrigation has moderated temperatures through latent heat flux changes (Cook *et al* 2015, Thiery *et al* 2017, Singh *et al* 2018), while deforestation has been linked to contrasting local and non-local climate changes (Christidis *et al* 2013, Findell *et al* 2017, Winckler *et al* 2019).

Of the many changes attributed to anthropogenic climate change, changes in compound events will contribute to some of the most severe societal and environmental impacts, but are still not well understood (Zscheischler *et al* 2020, Zhang *et al* 2021). Compound events can be defined as the combination of multiple climate processes associated with negative impacts (Zscheischler *et al* 2018), and those associated with extreme heat are especially significant (Mazdiyasni and AghaKouchak 2015, Li *et al* 2020). Compound hot and dry precipitation events have been shown to produce amplified impacts on ecosystem health and food production, and can lead to severe wildfires and power grid failures (Allen *et al* 2015, AghaKouchak *et al* 2020, Ribeiro *et al* 2020). Compound hot and humid conditions are also extremely dangerous for human health and can amplify heat-related morbidity and mortality rates (Li *et al* 2020, Raymond *et al* 2020). With future warming, compound hot events are expected to become more frequent and intense due to changing temperature distributions alongside changes in the dependencies of interrelated variables (Zscheischler *et al* 2020). Improving our understanding of compound hot events is therefore relevant for climate change preparedness. Critically, while daytime and nighttime temperatures are generally governed by the same overlying atmospheric conditions (Perkins 2015), different mechanisms may affect how these events respond to climate forcings. Daytime heat is often associated with dry soil moisture conditions, reduced cloud cover, and can be sensitive to land-atmosphere interactions; conversely, nighttime heat is typically associated with high humidity and increased cloud cover (Thomas *et al* 2020). It is therefore possible that daytime and nighttime compound heat responses may differ across anthropogenic forcings.

To study the individual contributions of each major anthropogenic forcing to changes in compound heat event occurrences, we used data from Goddard Institute for Space Studies (GISS) ModelE2.1-G Coupled Model Intercomparison Project: Phase 6 (CMIP6) Detection and Attribution Model Intercomparison Project (DAMIP) single-forcing runs (Gillett *et al* 2016). Using monthly maximum and minimum temperatures to represent daytime and nighttime temperatures, we examined four compound events representing 'warm-dry' (warm maximum/minimum temperature co-occurring with low precipitation) and 'warm-humid' (warm maximum/minimum temperature co-occurring with high specific humidity) conditions. We focused on meteorological drought and high humidity due to the severe environmental and agricultural impacts associated with these events (Madadgar *et al* 2017, Harpold and Brooks 2018, Matthews 2018). With these event pairs, we investigated how individual anthropogenic greenhouse gas, aerosol, and land-use/land-cover forcings affect the frequency of these compound events.

2. Methodology

2.1. Data

We used monthly maximum and minimum temperatures, precipitation, and specific humidity data from five ensemble members (r[1–5]i1p1f2) from GISS ModelE2.1-G CMIP6 DAMIP historical single-forcing runs from the most recent 60 years of available data, 1955–2014 (NASA/GISS 2018). The GISS Model E2.1-G is one of the latest configurations of the GISS ModelE for CMIP6, coupling the atmospheric general circulation model, ModelE, to the GISS ocean model to produce 2-by-2.5 degree resolution output. GISS ModelE2.1-G simulations have been shown to accurately simulate observed climate conditions and realistically respond to natural and anthropogenic climate forcings (Miller *et al* 2021, NASA/GISS 2018).

We used the historical natural-only (hist-nat) experiment, which includes only natural (solar, orbital, and volcanic aerosol) forcings, to find baseline estimates of compound event occurrences due to natural variability (Gillett *et al* 2016). We then investigated the effects of anthropogenic forcings on compound events by comparing hist-nat frequencies to four alternative experiments. The first three are single-forcing experiments: historical greenhouse gas-only (hist-GHG), anthropogenic aerosol-only (hist-aer), and historical land use-only (land-hist), which includes land cover (e.g. agricultural expansion) and irrigation changes (Cook *et al* 2015). The fourth experiment is the historical 'all-forcing' experiment, which includes natural forcings, ozone depletion, and all anthropogenic forcings from the three single-forcing experiments. We used the hist-nat experiment in lieu of the pre-industrial control (piControl) experiment to directly examine the contributions of anthropogenic forcings to the recent historical climate.

2.2. Parametric bivariate standardized index

For our study, we generated standardized precipitation indices (SPIs), standardized humidity indices (SHIs), and standardized maximum and minimum temperature indices (STIs), to calculate bivariate standardized indices and identify warm-dry and

warm-humid events. We used the entire calendar year to fully represent these events, as warm-dry and warm-humid conditions produce significant impacts in all seasons (Dierauer *et al* 2019, Ribeiro *et al* 2020). To construct the indices, we used a parametric approach and six month moving windows to capture medium-term moisture and heat events. For each grid cell, we pooled data from 1955 to 2014 from all hist-nat ensemble members to serve as the reference dataset for determining the appropriate distribution parameters so the standardized values are comparable across experiments.

For SPI, we calculated hist-nat six month moving sums and fit the pooled precipitation sums from each month to the appropriate gamma distribution (McKee *et al* 1993). We used the non-parametric Kolmogorov-Smirnov test to evaluate the goodness of fits of the selected distributions and found that more than 97% of months in all grid cells achieved adequate fits (Massey 1951). We then used each month's fitted distribution to approximate the cumulative probabilities associated with the precipitation sums from each experiment (historical, hist-nat, hist-GHG, hist-aer, and land-hist). We transformed the probabilities into standardized values with:

$$\mathrm{SPI} = \phi^{-1}(p) \tag{1}$$

where p is the cumulative probability of precipitation and ϕ is the standard normal distribution function.

For SHI and STI, we calculated six month moving averages for specific humidity, maximum and minimum temperature. We used appropriate beta distributions to construct the SHI index (Price 2001) and normal distributions to construct the STI index (Hansen *et al* 2012, Zscheischler *et al* 2014). For these indices, we found that greater than 98% of distributions achieved adequate fits. Then, as was done for SPI, we associated cumulative probabilities with the raw humidity and temperature values from each experiment and transformed the probabilities into standardized values with equation (1).

Following similar approaches used in the literature, we constructed the bivariate index with copula theory (Hao and AghaKouchak 2013, Li *et al* 2021). The copula is a multivariate distribution function which can model the dependence between multiple variables and can be used to study hydrometeorological multivariate dependencies (Michele and Salvadori 2003). With the VineCopula R package, we selected the copula with the lowest Bayesian information criterion and verified goodness-of-fit with White's information matrix equality to represent the dependence between the reference indices for each month of each grid cell (White 1982, Nagler *et al* 2019). We used *Gaussian, Clayton, Gumbel, Frank,* and *Joe* copulas, which have previously been used to represent the monthly bivariate dependencies (Sadegh *et al* 2017, Zscheischler and Seneviratne 2017, Li *et al* 2021). For months where the variables are statistically independent, we employed the *Independence* copula (Genest and Favre 2007). Based on Sklar's theorem, the joint cumulative distribution function F of STI (X) and SPI (Y) can be expressed in terms of a copula and its marginals:

$$F_{XY}(x,y) = C[F_X(x), F_Y(y)] \tag{2}$$

where C is the fitted copula's cumulative distribution function, and $F_X(x)$ and $F_Y(y)$ represent the marginal cumulative distribution functions of STI and SPI where $F_X(x) = P(X \leqslant x)$ and $F_Y(x) = P(Y \leqslant y)$ (Sklar 1959).

The joint cumulative probability of warm and dry conditions can be calculated with:

$$P = \Pr(X \leqslant x, Y > y) = u - C(u,v) \tag{3}$$

where u and v are the univariate temperature and precipitation probabilities.

The joint cumulative probability of warm and humid conditions can be calculated with:

$$P = \Pr(X \leqslant x, Y \leqslant y) = C(u,v) \tag{4}$$

where u and v are the temperature and humidity probabilities. Finally, to generate our bivariate indices, we transformed the joint cumulative probabilities into standardized values with equation (1).

2.3. Compound event analysis

Using our bivariate indices, we identified compound warm-dry and warm-humid events as consecutive months exceeding the 90th percentile of the cumulative joint probability. Our primary analysis examined the frequency of compound events during 1955–2014. In the supplemental materials, we compare ModelE2.1-G historical output to the Modern-Era Retrospective Analysis for Research and Applications, Version 2 (MERRA-2) reanalysis data to demonstrate that ModelE2.1-G adequately represents the frequencies of these compound events (SM figure 1). In addition, we examined how the compound events are zonally distributed by pooling land grid cells from all ensemble members in each latitude band. We additionally pooled each SREX region's land grid cells from all ensemble members and evaluated median differences from the hist-nat baseline with Mood's median test using an alpha of 0.05 (Mood 1950, Field *et al* 2012). In the supplemental materials, we include plots of compound event duration and intensity, defining duration as the number of months and intensity as the sum of standardized values associated with each event (SM figures 2–7) and results using 3- and 12 month moving windows as well as 80th and 95th percentile thresholds (SM figures 8–15). We also examined how anthropogenic forcings have impacted the background climate conditions during 1955–2014 to provide additional context for our results.

3. Results

3.1. Global evaluation of compound warm events

Here, we first examine the global frequency of compound warm-dry and warm-humid events in the hist-nat experiment in 1955–2014 (figure 1). In the absence of anthropogenic forcings, warm-dry events are mostly found in tropical and extratropical regions, while warm-humid events occur more frequently in the higher latitudes. These distributions reflect the strengths of the dependencies between warm and dry conditions and warm and humid conditions due to natural variability, and have been shown in observations (Dai 2006, Zscheischler and Seneviratne 2017) and in MERRA-2 (SM figure 1). In hist-nat conditions, daytime (Tmax) warm-dry events occur more frequently relative to nighttime (Tmin) warm-dry events in most regions. In contrast, nighttime warm-humid events are more frequent relative to daytime warm-humid events across the globe. These dissimilarities may stem from underlying differences in the drivers of daytime and nighttime high temperatures. As previously mentioned, daytime heat is generally associated with dry land surface conditions and low cloud cover, while nighttime heat has been connected to high humidity and cloud cover (Thomas *et al* 2020).

In general, daytime and nighttime warm-dry events have similar responses to the individual forcings (figure 2). Compared to hist-nat conditions, greenhouse gases (figures 2(e) and (f)) drive large-scale increases in event frequency, while anthropogenic aerosols and land-use/land-cover changes (figures 2(i), (j), (m) and (n)) cause broad decreases. In the hist-GHG experiment, tropical and extratropical regions display the largest increases in daytime and nighttime warm-dry events, amplifying hist-nat baseline frequency patterns. In the hist-aer experiment, the hist-nat frequencies of daytime and nighttime warm-dry events are suppressed by aerosols. Meanwhile, most regions do not show significant warm-dry changes in land-hist. In the historical experiment (figures 2(a) and (b)), the combination of these individual forcings strikingly results in modest decreases in daytime warm-dry events relative to hist-nat conditions in the Northern Hemisphere, as well as substantial increases in the Southern Hemisphere for both event types.

For daytime and nighttime warm-humid events, we also see general event frequency increases in the hist-GHG experiment (figures 2(g) and (h)) and decreases in the hist-aer and land-hist experiments (figures 2(k), (l), (o) and (p)). The presence of greenhouse gases amplifies the hist-nat frequency of warm-humid events, resulting in large increases in the Northern polar regions, as well as increases in the tropics and extratropics (e.g. North America, Sub-Saharan Africa, Europe, and East Asia) where high frequencies of nighttime warm-humid events occur under hist-nat baseline conditions. However, the presence of aerosols and land-use/land-cover change also substantially impacts the Northern polar regions. Consequentially, in the historical experiment, we see increases concentrated in the tropics and extratropics relative to the baseline (figures 2(c) and (d)). Overall, we see a greater absolute increase in nighttime warm-humid events in the historical experiment, especially in tropical and polar latitudes, reflecting differences in the responses of daytime and nighttime events to the combination of anthropogenic forcings.

3.2. Latitudinal and regional evaluation of compound events

To summarize the global results, we provide pooled ensemble median and interquartile ranges of event frequency across latitude bands for the forced experiments relative to the hist-nat baseline (figure 3). For compound warm-dry conditions, daytime and nighttime events generally display similar patterns, with the median hist-GHG event frequency increasing by approximately 150%–500% in the tropics and extratropics (40° N–40° S) and the hist-aer event frequency experiencing declines ranging from 60% to 100% in similar latitudes (figures 3(a) and (b)). Events also substantially decline in the land-hist experiment, although aerosols provide a stronger dampening effect across almost all latitude bands. With these plots, we can also highlight the strong impact of aerosols on daytime events, with historical daytime events being noticeably reduced by 30%–50% relative to the baseline at 35°–55° N. The latitudinal profiles of warm-humid events also display the strong effect of greenhouse gases, with increases ranging from 200% to 900% across most latitudes between 40° N–40° S (figures 3(c) and (d)). Meanwhile, historical warm-humid events are strongly moderated by aerosols and land-use/land-cover change, resulting in more modest increases between 100% and 300% in similar latitudes.

Next, we use boxplots to show compound event frequency distributions in select regions. We display results from Central North America (CNA), Central Europe (CEU), South Asia (SAS), East Asia (EAS), the Amazon (AMZ), and East Africa (EAS) to present a range of climate regions across the globe. Greenhouse gases significantly increase the hist-nat baseline median of daytime warm-dry events by approximately 200%–350% for all regions presented (figure 4(a)). Meanwhile, aerosol and land-use/land-cover change significantly decrease daytime warm-dry event frequency, reducing the median frequency to 0 in most regions. As demonstrated with figure 3, we can see the strong moderating effect of aerosols and land-use/land-cover on the historical daytime warm-dry events in Northern Hemisphere regions (CNA, CEU, SAS, and EAS), resulting in 25%–50% median decreases relative to

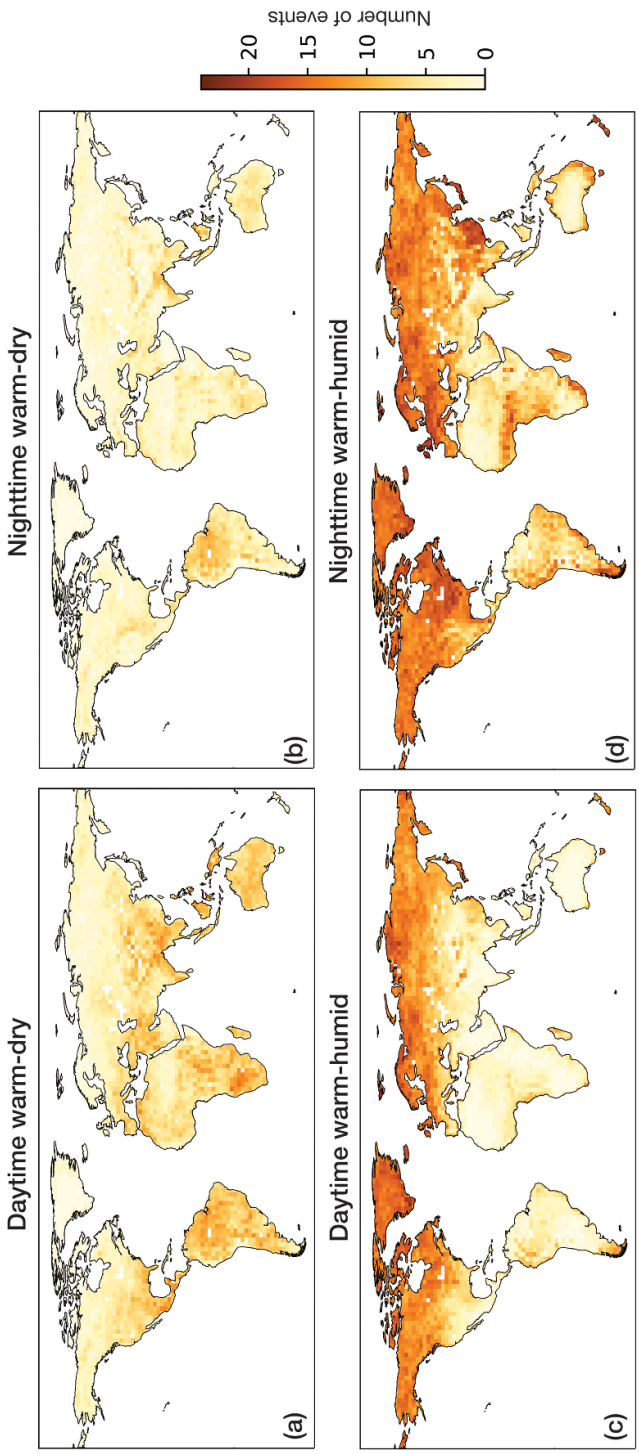

Figure 1. GISS ModelE2.1-G r[1–5]i1p1f2 historical natural-only global distributions of warm-dry and warm-humid 1955–2014 event frequency with events based on a 90th percentile threshold. (a) Ensemble median daytime (T_{max}) warm and dry events (units are number of events). (b) Median nighttime (T_{min}) warm and dry events. (c) Median daytime warm and humid events. (d) Median nighttime warm and humid events.

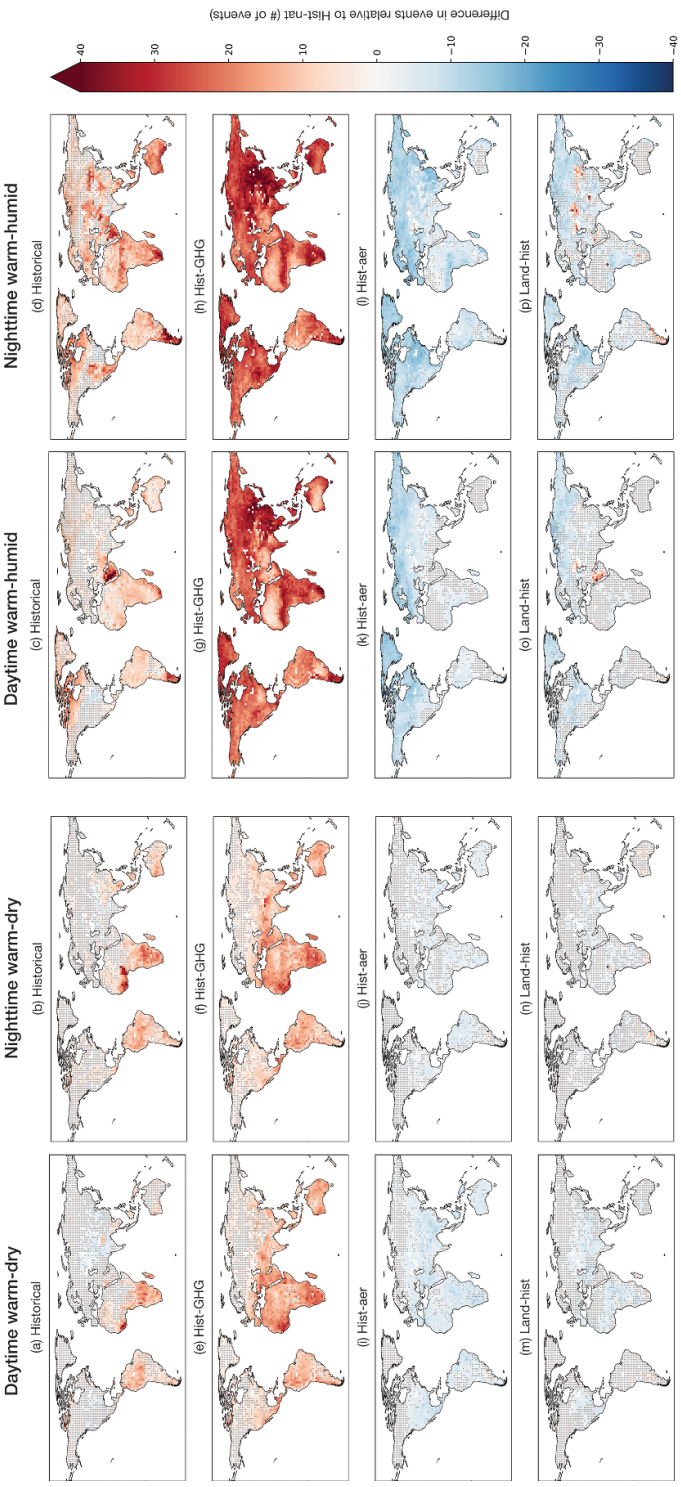

Figure 2. GISS ModelE2.1-G r[1–5]i1p1f2 forced difference in warm-dry and warm-humid 1955–2014 event frequency relative to historical natural-only conditions with events based on a 90th percentile threshold. Each column presents the historical, hist-GHG, hist-aer, and land-hist difference in the event frequency relative to the historical natural-only event frequency (units in number of events). Grid cells where not all ensemble members agree on the sign of the forced event frequency difference relative to hist-nat are hatched.

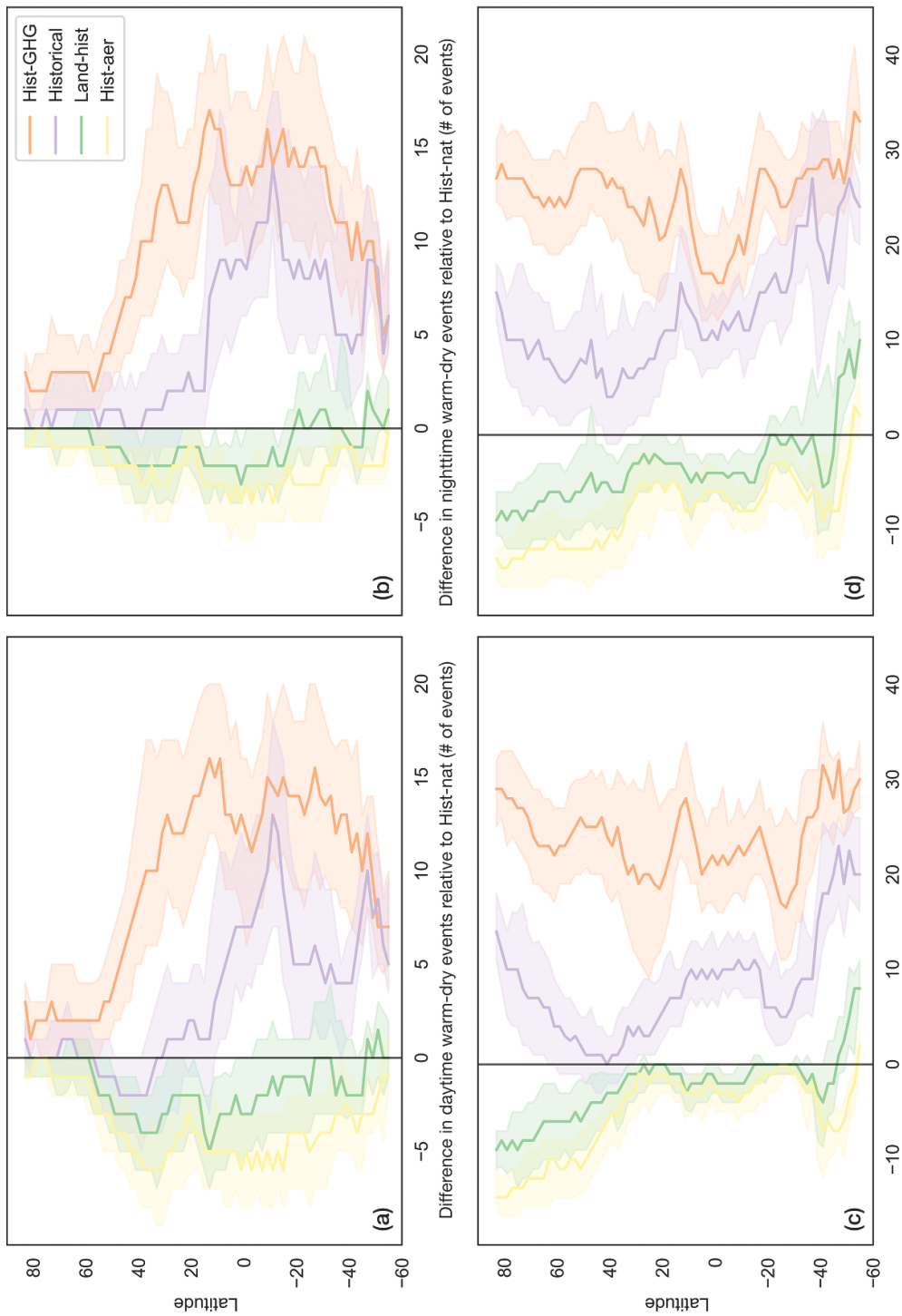

Figure 3. Latitudinal distributions of differences in warm-dry and warm-humid event frequency relative to historical natural-only conditions based on GISS ModelE2.1-G r[1–5]i1p1f2 simulations. (a) Pooled ensemble median and interquartile range (IQR) for daytime warm and dry event frequency at each latitude band for historical, hist-GHG, hist-aer, and land-hist (units in number of events). (b) Pooled ensemble median and IQR for nighttime warm and dry event frequency. (c) Pooled ensemble median and IQR for daytime warm and humid event frequency. (d) Pooled ensemble median and IQR for nighttime warm and humid event frequency.

the baseline. In contrast, the historical warm-dry frequency is significantly higher than the hist-nat frequency in the Southern Hemisphere (AMZ, EAF), due to the reduced contribution of aerosols and land-use/land-cover to the historical event frequency in these regions. Greenhouse gases also increase nighttime warm-dry events by approximately 300%–500% for all regions relative to the hist-nat (figure 4(b)). In addition, aerosols and land-use/land-cover changes also provide a moderating effect on the historical event frequency in the Northern regions. However, in contrast to daytime conditions, we still see evidence of significant increases in nighttime warm-dry events under historical conditions, with increases ranging from 30% to 300% in most regions (excluding SAS).

Daytime (figure 4(c)) and nighttime (figure 4(d)) warm-humid events also show consistently large event frequency increases with the hist-GHG forcing, which highlight the far-reaching impact of greenhouse gases. In the hist-aer experiment, we can see the almost complete suppression of warm-humid event frequency, highlighting the joint effect of cooling and drying from aerosols. Although land-use/land-cover changes provide more moderate reductions in warm-humid events, regional event frequencies are still significantly different from hist-nat conditions. Overall, between daytime and nighttime warm-humid events, the frequency of nighttime events is still substantially higher under historical conditions, amplifying the underlying hist-nat patterns.

3.3. Background climate conditions

To provide context for how anthropogenic activity has influenced these events, we examine how the forcings have impacted average climate conditions. In general, responses in average maximum and minimum temperature are similar to the compound event responses, with broad temperature increases in hist-GHG conditions and decreases in hist-aer and land-hist (figure 5). In the hist-aer experiment, we see evidence that maximum temperature is more sensitive to aerosols, resulting in a greater decrease in maximum relative to minimum temperature, especially in the Northern Hemisphere. In the historical experiment, we can further highlight the differences between maximum and minimum temperature in the Northern Hemisphere, underscoring the stronger impact of aerosols on maximum temperatures. The different sensitivities of maximum and minimum temperature to aerosols are present in the compound responses to the anthropogenic forcings, and is especially noticeable for warm-dry events. In the land-hist experiment, we also see local mid-latitude and non-local upper-latitude declines in both maximum and minimum temperature stemming from native vegetation loss and irrigation activity, agreeing with previous findings (Singh *et al* 2018). Although land-use/land-cover drive both local and non-local changes, these changes are not as widespread and are generally more modest compared to aerosol-driven changes, apart from the irrigation-driven cooling of the Indo-Gangetic Plain (Puma and Cook 2010, Singh *et al* 2018).

We also examine how average precipitation, specific humidity, and cloud area fraction have responded to the individual forcings (figure 6). Under hist-GHG conditions, there are average precipitation increases in the higher latitudes and decreases in the Mediterranean, Northern Africa, the Middle East, and Central America. Coupled with changes in average temperature, the tropical and extratropical areas of concurrent robust drying and warming correspond well with where warm-dry events increase under greenhouse gas conditions. In the hist-aer experiment, we see a general drying effect stemming from aerosols; however, due to associated significant large-scale decreases in temperature, drying from aerosols does not meaningfully increase warm-dry events on an individual basis. Meanwhile, although land-use/land-cover change produces a strong regional wetting signal in parts of Northern Africa and the Middle East, this ultimately does not result in significant changes in warm-dry events.

Changes in average specific humidity are more widespread: specific humidity increases globally in the hist-GHG experiment, and decreases in the hist-aer and land-hist experiments. With greenhouse gases, concurrent increases in specific humidity and temperature directly increase the number of warm-humid events across the globe shown in figure 2. Meanwhile, aerosols and land-use/land-cover change generally provide both cooler and drier conditions that moderate the frequency of warm-humid events relative to warm-dry events.

Differences in average cloud area fraction strongly relate to average maximum and minimum temperatures, and contribute to the overall differences between daytime and nighttime compound events. Relative to hist-nat conditions, increases in historical cloud area fraction are most influenced by the presence of aerosols. As cloud area fraction provides a much stronger effect on daytime temperatures, maximum temperature is more sensitive to this forcing, contributing to the identified differences in daytime and nighttime event responses.

Ultimately, this analysis of average climate conditions reveals the contributing factors driving changes in compound warm-dry and warm-humid event frequency. Under hist-GHG conditions, tropical and extratropical regions experiencing concurrent warming and drying show pronounced increases in warm-dry events, while aerosols and land-use/land-cover changes moderate these increases through their influences on temperature. Greenhouse gases also produce substantial increases in warm-humid events by influencing both average temperature and specific

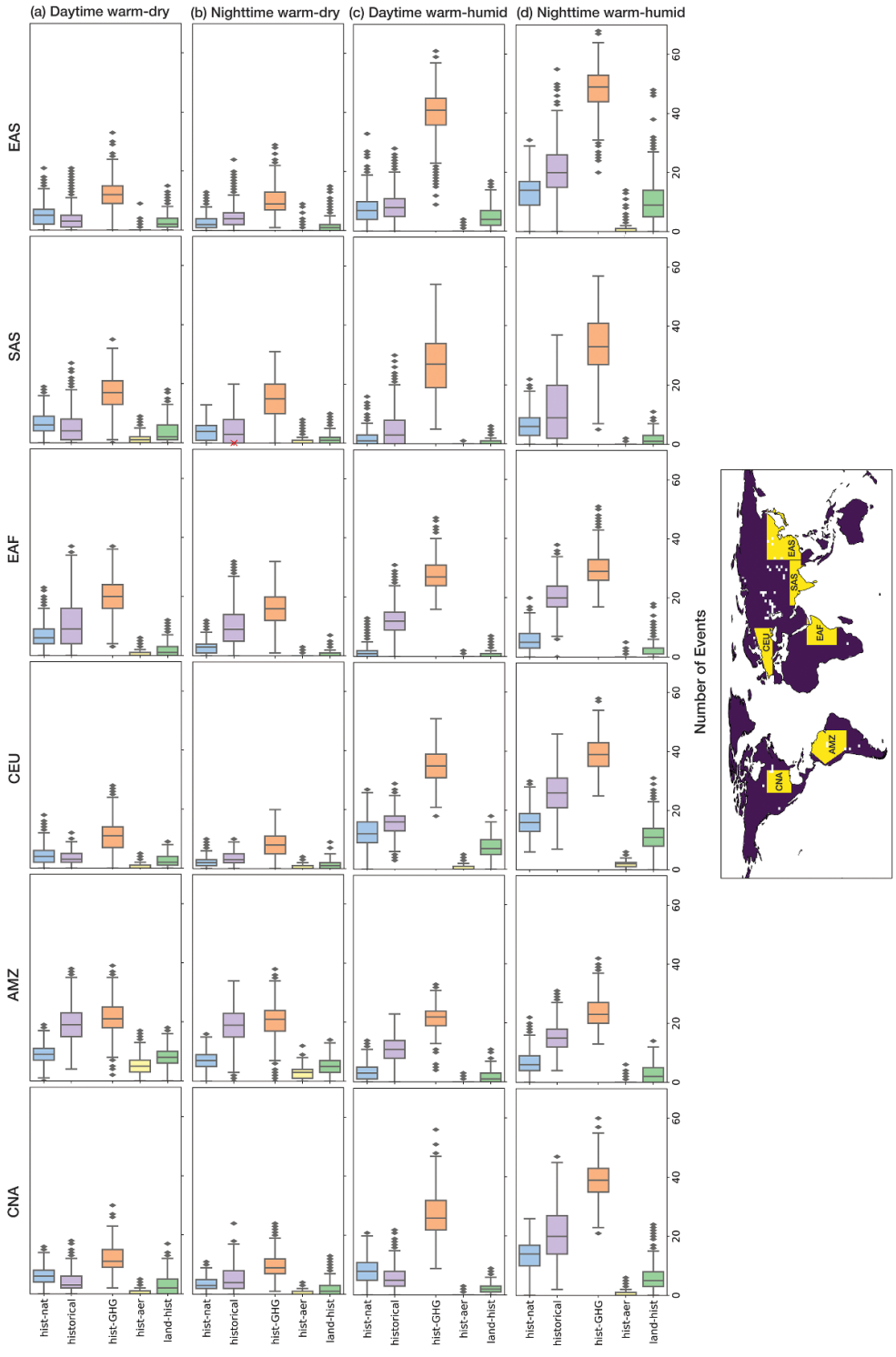

Figure 4. Pooled ensemble event frequency boxplots based on GISS ModelE2.1-G r[1–5]i1p1f2 simulations. Each boxplot displays the distribution of grid cells within a given region under the specified experiment (units in number of events) and for each event type. Regions displayed: Central North America (CNA), Central Europe (CEU), South Asia (SAS), East Asia (EAS), Amazon (AMZ), and East Africa (EAF). The red *x* mark indicates that the nighttime warm-dry historical median from the SAS region is not significantly different from the corresponding historical natural-only median. All other forced medians are significantly different from the historical natural-only median.

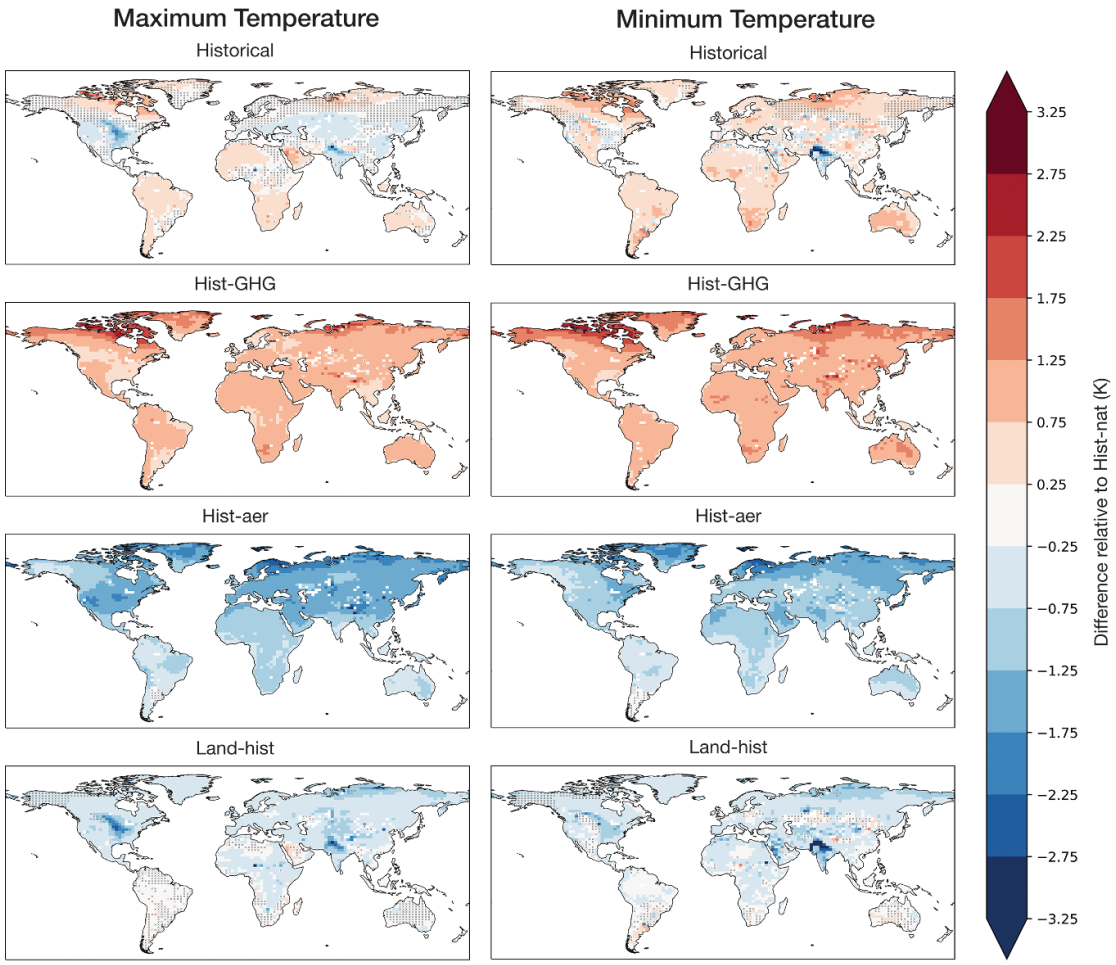

Figure 5. Forced differences in average maximum and minimum temperatures relative to historical natural-only conditions in 1955–2014 based on GISS ModelE2.1-G r[1–5]i1p1f2 simulations. Each column presents the historical, hist-GHG, hist-aer, and land-hist absolute difference in average monthly temperature relative to historical natural-only conditions. Grid cells where not all ensemble members agree on the sign of the forced difference relative to hist-nat are hatched.

humidity. Nevertheless, these same events are moderated strongly by the presence of aerosols and land-use/land-cover changes that cause concurrent declines in temperature and specific humidity. Differences in daytime and nighttime compound event frequencies are influenced by differences in day and night temperature responses to cloud area fraction, generally resulting in larger increases in historical nighttime compound events relative to the hist-nat baseline.

4. Discussion

Under warming temperatures, compound events will produce severe impacts across sectors. Previous studies have documented how compound warm-dry and warm-humid events have and will continue to increase due to climate change, but have not delved into how individual anthropogenic forcings contribute to the occurrence of these events (Zscheischler and Seneviratne 2017, Li *et al* 2020). Additionally, the degree to which these events will change in response to anthropogenic forcings, and the underlying mechanisms driving these changes, is not well understood. Most studies have also used average or maximum temperature to represent compound hot events (Alizadeh *et al* 2020), and have not examined how compound events defined by nighttime temperatures may respond differently.

Here, we conducted a comprehensive analysis of the effects of greenhouse gases, aerosols, and land-use/land-cover change on daytime and nighttime warm-dry and warm-humid events. Greenhouse gases increase warm-dry event frequencies in tropical and extratropical latitudes through large-scale daytime and nighttime temperature increases, while aerosols and land-use/land-cover changes reduce warm-dry event frequencies in similar latitudes through cooling. In the historical experiment, we see net decreases in daytime warm-dry events in the Northern mid-latitudes, and net increases in both daytime and nighttime warm-dry events in the Southern Hemisphere. Meanwhile, greenhouse gases substantially amplify warm-humid event frequencies

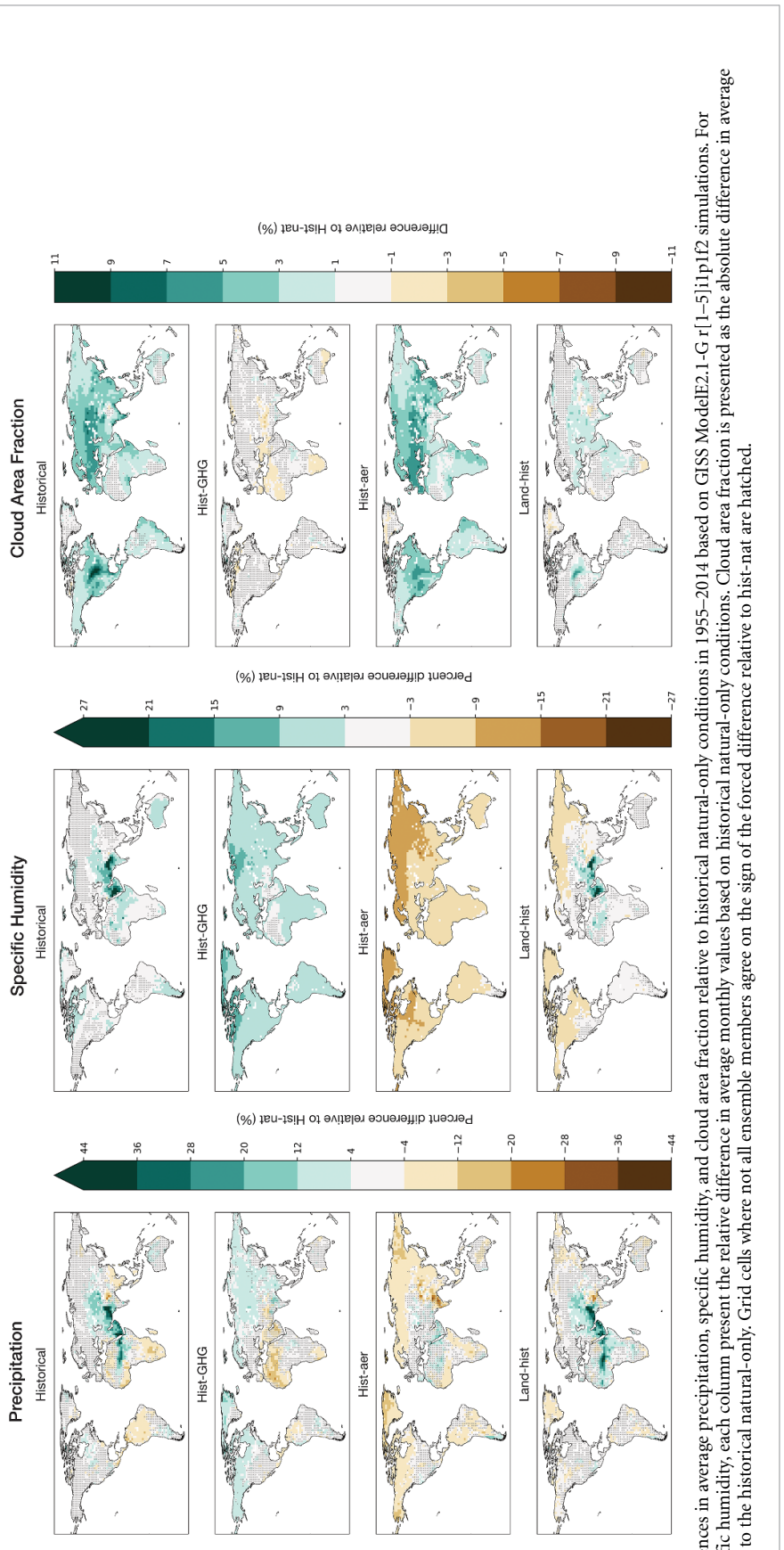

Figure 6. Forced differences in average precipitation, specific humidity, and cloud area fraction relative to historical natural-only conditions in 1955–2014 based on GISS ModelE2.1-G r[1–5]i1p1f2 simulations. For precipitation and specific humidity, each column present the relative difference in average monthly values based on historical natural-only conditions. Cloud area fraction is presented as the absolute difference in average monthly values relative to the historical natural-only. Grid cells where not all ensemble members agree on the sign of the forced difference relative to hist-nat are hatched.

in tropical, extratropical, and polar regions, while aerosols and land-use/land-cover changes considerably dampen warm-humid events in the Northern polar regions. Overall, we see net increases in historical daytime and nighttime warm-humid events across most latitudes, although we see larger increases in the Southern Hemisphere.

Our results generally agree with established temperature, precipitation, and humidity changes associated with greenhouse gas and aerosol emissions. Previous studies have tied global temperature and specific humidity increases and regional drying patterns from dynamic and thermodynamic changes in the hydrological cycle to greenhouse gases (Seager *et al* 2010, Marvel and Bonfils 2013). Large-scale cooling and drying from aerosols has also been well established, and GISS E2.1 G has been shown to produce similar temperature responses to aerosols relative to the CMIP6 multi-model mean; however, there are still existing model biases related to aerosols (Tokarska *et al* 2020). With regards to land-use/land-cover changes, our results agree with previous studies that have attributed cooling to native vegetation loss and irrigation increases (Pitman *et al* 2012, Christidis *et al* 2013). However, this stands in contrast to studies which have identified forest loss-related regional warming signals (Alkama and Cescatti 2016, Findell *et al* 2017). These discrepancies may stem from model assumptions regarding non-radiative land cover characteristics (Bright *et al* 2017) and observational underestimations of non-local surface cooling (Winckler *et al* 2019).

Overall, substantial differences between daytime and nighttime compound events emerge in the historical experiment that can be traced back to the individual forcings. Due to the impacts of aerosols and associated cloud cover increases on maximum temperature, we even see historical decreases in the frequency of daytime warm-dry events in the Northern Hemisphere. The temperature responses seen here agree with previous studies investigating diurnal temperature changes (Hansen *et al* 1995).

Although CMIP models produce temperature-precipitation and temperature-humidity dependence patterns similar to observations, we acknowledge that the strengths of the dependencies are overstated in most models, including GISS (Dunn *et al* 2017). Most CMIP6 models also underestimate the diurnal temperature range relative to observations due to aerosol and cloud model biases, which can be reflected in our results (Wang and Clow 2020). Precipitation and humidity biases in GISS ModelE2.1 may also impact our results (Kelley *et al* 2020). Separately, we acknowledge that the methodological choices we have made can also influence our results. For example, using alternative models with different representations of land-atmosphere coupling may impact these compound events and how sensitive they may be to the various forcings.

5. Conclusion

We have demonstrated how anthropogenic forcings influence daytime and nighttime warm-dry and warm-humid events at regional and global scales. By examining the single-forcing experiments, we have characterized how responses in average climate conditions contribute to differences in event frequencies. Because daytime and nighttime compound events can lead to distinct impacts, our analysis offers a more comprehensive assessment of current and future compound event risks to human health, ecosystem health, and infrastructure. As greenhouse gas emissions are expected to continue impacting our global climate, we expect to see greater frequencies of warm-dry and especially warm-humid events. Additionally, due to the expected 21st century decline in anthropogenic aerosols, we may expect to see even greater increases in daytime and nighttime warm-dry and warm-humid conditions.

Data availability statement

The data that support the findings of this study are openly available at the following URL/DOI: https://doi.org/10.22033/ESGF/CMIP6.1400.

Acknowledgments

B I Cook, K Marvel, G A Schmidt, L S Nazarenko, and M Kelly were all supported by NASA's Modeling, Analysis, and Prediction program. F Chiang was supported by an appointment to the NASA Postdoctoral Program at the NASA Goddard Institute for Space Studies, administered by Universities Space Research Association and Oak Ridge Associated Universities under contracts with NASA. Resources supporting this work were provided by the NASA High-End Computing (HEC) Program through the NASA Center for Climate Simulation (NCCS) at Goddard Space Flight Center. The views and conclusions contained in this article are those of the authors and should not be interpreted as representing the official policies, either expressed or implied, of NASA or the U.S. Government. The U.S. Government is authorized to reproduce and distribute reprints for Government purposes notwithstanding any copyright notation herein.

ORCID iD

Felicia Chiang https://orcid.org/0000-0003-4191-6157

References

AghaKouchak A, Chiang F, Huning L S, Love C A, Mallakpour I, Mazdiyasni O, Moftakhari H, Papalexiou S M, Ragno E and Sadegh M 2020 Climate extremes and compound hazards in a warming world *Annu. Rev. Earth Planet. Sci.* **48** 519–48

Alizadeh M R, Adamowski J, Nikoo M R, AghaKouchak A, Dennison P and Sadegh M 2020 A century of observations reveals increasing likelihood of continental-scale compound dry-hot extremes *Sci. Adv.* **6** eaaz4571
Alkama R and Cescatti A 2016 Biophysical climate impacts of recent changes in global forest cover *Science* **351** 600–4
Allen C D, Breshears D D and McDowell N G 2015 On underestimation of global vulnerability to tree mortality and forest die-off from hotter drought in the anthropocene *Ecosphere* **6** art129
Bollasina M A, Ming Y and Ramaswamy V 2011 Anthropogenic aerosols and the weakening of the South Asian Summer Monsoon *Science* **334** 502–5
Bright R M, Davin E, O'Halloran T, Pongratz J, Zhao K and Cescatti A 2017 Local temperature response to land cover and management change driven by non-radiative processes *Nat. Clim. Change* **7** 296–302
Charlson R J, Schwartz S E, Hales J M, Cess R D, Coakley J A, Hansen J E and Hofmann D J 1992 Climate forcing by anthropogenic aerosols *Science* **255** 423–30
Christidis N, Stott P A, Brown S, Hegerl G C and Caesar J 2005 Detection of changes in temperature extremes during the second half of the 20th century *Geophys. Res. Lett.* **32** 20
Christidis N, Stott P A, Hegerl G C and Betts R A 2013 The role of land use change in the recent warming of daily extreme temperatures *Geophys. Res. Lett.* **40** 589–94
Cook B I, Shukla S P, Puma M J and Nazarenko L S 2015 Irrigation as an historical climate forcing *Clim. Dyn.* **44** 1715–30
Dai A 2006 Recent climatology, variability, and trends in global surface humidity *J. Clim.* **19** 3589–606
Dierauer J R, Allen D M and Whitfield P H 2019 Snow drought risk and susceptibility in the Western United States and Southwestern Canada *Water Resour. Res.* **55** 3076–91
Dunn R J H, Willett K M, Ciavarella A and Stott P A 2017 Comparison of land surface humidity between observations and CMIP5 models *Earth Syst. Dyn.* **8** 719–47
Easterling D R, Kunkel K E, Wehner M F and Sun L 2016 Detection and attribution of climate extremes in the observed record *Weather Clim. Extremes* **11** 17–27
Field C B, Barros V, Stocker T F and Dahe Q 2012 *Managing the Risks of Extreme Events and Disasters to Advance Climate Change Adaptation: Special Report of the Intergovernmental Panel on Climate Change* (Cambridge: Cambridge University Press)
Findell K L, Berg A, Gentine P, Krasting J P, Lintner B R, Malyshev S, Santanello J A and Shevliakova E 2017 The impact of anthropogenic land use and land cover change on regional climate extremes *Nat. Commun.* **8** 1–10
Genest C and Favre A-C 2007 Everything you always wanted to know about copula modeling but were afraid to ask *J. Hydrol. Eng.* **12** 347–68
Gillett N P, Shiogama H, Funke B, Hegerl G, Knutti R, Matthes K, Santer B D, Stone D and Tebaldi C 2016 The detection and attribution model intercomparison project (DAMIP v1.0) contribution to CMIP6 *Geosci. Model Dev.* **9** 3685–97
Hansen J, Sato M and Ruedy R 1995 Long-term changes of the diurnal temperature cycle: implications about mechanisms of global climate change *Atmos. Res.* **37** 175–209
Hansen J, Sato M and Ruedy R 2012 Perception of climate change *Proc. Natl Acad. Sci.* **109** E2415–23
Hao Z and AghaKouchak A 2013 Multivariate standardized drought index: a parametric multi-index model *Adv. Water Resour.* **57** 12–18
Harpold A A and Brooks P D 2018 Humidity determines snowpack ablation under a warming climate *Proc. Natl Acad. Sci.* **115** 1215–20
Hegerl G C, Hasselmann K, Cubasch U, Mitchell J F B, Roeckner E, Voss R and Waszkewitz J 1997 Multi-fingerprint detection and attribution analysis of greenhouse gas, greenhouse gas-plus-aerosol and solar forced climate change *Clim. Dyn.* **13** 613–34
IPCC 2021 Climate change 2021: the physical science basis *Contribution of Working Group I to the Sixth Assessment Report of the Intergovernmental Panel on Climate Change* ed V Masson-Delmotte *et al* (Cambridge: Cambridge University Press)
Kelley M *et al* 2020 GISS-E2.1: configurations and climatology *J. Adv. Model. Earth Syst.* **12** e2019MS002025
Li D, Yuan J and Kopp R E 2020 Escalating global exposure to compound heat-humidity extremes with warming *Environ. Res. Lett.* **15** 064003
Li J, Wang Z, Wu X, Zscheischler J, Guo S and Chen X 2021 A standardized index for assessing sub-monthly compound dry and hot conditions with application in China *Hydrol. Earth Syst. Sci.* **25** 1587–601
Madadgar S, AghaKouchak A, Farahmand A and Davis S J 2017 Probabilistic estimates of drought impacts on agricultural production *Geophys. Res. Lett.* **44** 7799–807
Marvel K and Bonfils C 2013 Identifying external influences on global precipitation *Proc. Natl Acad. Sci.* **110** 19301–6
Marvel K, Cook B I, Bonfils C J W, Durack P J, Smerdon J E and Williams A P 2019 Twentieth-century hydroclimate changes consistent with human influence *Nature* **569** 59–65
Massey F J 1951 The kolmogorov-smirnov test for goodness of fit *J. Am. Stat. Assoc.* **46** 68–78
Matthews T 2018 Humid heat and climate change *Prog. Phys. Geogr.* **42** 391–405
Mazdiyasni O and AghaKouchak A 2015 Substantial increase in concurrent droughts and heatwaves in the United States *Proc. Natl Acad. Sci.* **112** 11484–9
McKee T B, Doesken N J and Kleist J 1993 The relationship of drought frequency and duration to time scales *Proc. 8th Conf. on Applied Climatology* (Boston, MA: American Meteorological Society) pp 179–84
Michele C D and Salvadori G 2003 A generalized pareto intensity-duration model of storm rainfall exploiting 2-Copulas *J. Geophys. Res.* **108** 4067
Miller R L *et al* 2021 CMIP6 historical simulations (1850–2014) with GISS-E2.1 *J. Adv. Model. Earth Syst.* **13** e2019MS002034
Mood A M 1950 Introduction to the theory of statistics
Nagler T *et al* 2019 VineCopula: statistical inference of vine copulas (available at: https://CRAN.R-project.org/package=VineCopula)
NASA Goddard Institute for Space Studies (NASA/GISS) 2018 *NASA-GISS GISS-E2.1G Model Output Prepared for CMIP6 CMIP* (Earth System Grid Federation) (https://doi.org/10.22033/ESGF/CMIP6.1400)
Perkins S E 2015 A review on the scientific understanding of heatwaves—their measurement, driving mechanisms, and changes at the global scale *Atmos. Res.* **164–165** 242–67
Pitman A J *et al* 2012 Effects of land cover change on temperature and rainfall extremes in multi-model ensemble simulations *Earth Syst. Dyn.* **3** 213–31
Polson D, Bollasina M, Hegerl G C and Wilcox L J 2014 Decreased monsoon precipitation in the northern hemisphere due to anthropogenic aerosols *Geophys. Res. Lett.* **41** 6023–9
Price J D 2001 A study of probability distributions of boundary-layer humidity and associated errors in parametrized cloud-fraction *Q. J. R. Meteorol. Soc.* **127** 739–58
Puma M J and Cook B I 2010 Effects of irrigation on global climate during the 20th century *J. Geophys. Res.* **115** D16
Raymond C, Matthews T and Horton R M 2020 The emergence of heat and humidity too severe for human tolerance *Sci. Adv.* **6** eaaw1838
Ribeiro A F S, Russo A, Gouveia C M, Páscoa P and Zscheischler J 2020 Risk of crop failure due to compound dry and hot extremes estimated with nested copulas *Biogeosciences* **17** 4815–30
Sadegh M, Ragno E and AghaKouchak A 2017 Multivariate copula analysis toolbox (MvCAT): describing dependence and underlying uncertainty using a Bayesian framework *Water Resour. Res.* **53** 5166–83

Seager R, Naik N and Vecchi G A 2010 Thermodynamic and dynamic mechanisms for large-scale changes in the hydrological cycle in response to global warming *J. Clim.* **23** 4651–68

Seneviratne S I *et al* 2012 Changes in climate extremes and their impacts on the natural physical environment *Managing the Risks of Extreme Events and Disasters to Advance Climate Change Adaptation* ed C B Field, V Barros, T F Stocker and Q Dahe (Cambridge: Cambridge University Press) pp 109–230 (available at: www.cambridge.org/core/product/identifier/CBO9781139177245A030/type/book_part)

Singh D, McDermid S P, Cook B I, Puma M J, Nazarenko L and Kelley M 2018 Distinct influences of land cover and land management on seasonal climate *J. Geophys. Res.* **123** 12,017–12,039

Sklar M 1959 Fonctions de repartition a n dimensions et leurs marges *Publ. Inst. Statist. Univ. Paris* **8** 229–31

Thiery W, Davin E L, Lawrence D M, Hirsch A L, Hauser M and Seneviratne S I 2017 Present-day irrigation mitigates heat extremes *J. Geophys. Res.* **122** 1403–22

Thomas N P, Bosilovich M G, Collow A B M, Koster R D, Schubert S D, Dezfuli A and Mahanama S P 2020 Mechanisms associated with daytime and nighttime heat waves over the contiguous United States *J. Appl. Meteorol. Climatol.* **59** 1865–82

Tokarska K B, Stolpe M B, Sippel S, Fischer E M, Smith C J, Lehner F and Knutti R 2020 Past warming trend constrains future warming in CMIP6 models *Sci. Adv.* **6** eaaz9549

Wang K and Clow G D 2020 The diurnal temperature range in CMIP6 models: climatology, variability, and evolution *J. Clim.* **33** 8261–79

White H 1982 Maximum likelihood estimation of misspecified models *Econometrica* **50** 1–25

Winckler J, Lejeune Q, Reick C H and Pongratz J 2019 Nonlocal effects dominate the global mean surface temperature response to the biogeophysical effects of deforestation *Geophys. Res. Lett.* **46** 745–55

Zhang W, Luo M, Gao S, Chen W, Hari V and Khouakhi A 2021 Compound hydrometeorological extremes: drivers, mechanisms and methods *Front. Earth Sci.* **9** 941

Zscheischler J *et al* 2014 Impact of large-scale climate extremes on biospheric carbon fluxes: an intercomparison based on MsTMIP data *Glob. Biogeochem. Cycles* **28** 585–600

Zscheischler J *et al* 2018 Future climate risk from compound events *Nat. Clim. Change* **8** 469

Zscheischler J *et al* 2020 A typology of compound weather and climate events *Nat. Rev. Earth Environ.* **1** 333–47

Zscheischler J and Seneviratne S I 2017 Dependence of drivers affects risks associated with compound events *Sci. Adv.* **3** e1700263